

Computation of 3D Flows with Violent Free Surface Motion

Chi Yang¹ and Rainald Löhner

School of Computational Sciences, George Mason University
Fairfax, Virginia, U.S.A.

ABSTRACT

A robust Volume of Fluid (VOF) technique is presented together with an incompressible Euler/Navier Stokes solver operating on adaptive, unstructured grids to simulate the interactions of extreme waves and three-dimensional structures. The incompressible Euler/Navier Stokes equations are solved using projection schemes and a finite element method. The classic breaking dam problem is first used to validate the three-dimensional computer code developed based on the method described above. The computer code is then used to simulate the sloshing of a partially filled two-dimensional tank due to sway excitation. The resulting wave heights and pressure forces for various excitation frequencies and amplitudes are compared with experimental data and those predicted by the SPH method. The numerical simulation of the sloshing of a partially filled three-dimensional tank is carried out and compared with its counterpart of a two-dimensional tank. The computational results demonstrate that the present CFD method is capable of simulating the violent resonant free surface flows with strong nonlinear behavior in a partially filled tank, which is of great importance to the offshore and shipping industry.

KEY WORDS: Finite element method, VOF method, violent free surface flows, sloshing, nonlinear hydrodynamics, wave loading.

INTRODUCTION

In rough seas, ships or offshore structures may experience highly nonlinear phenomena such as slamming and green water on deck. Impact loads due to slamming and green water shipping are associated with the three dimensional flows with a violent free surface. A ship carrying liquid cargo in partially filled tanks in waves may experience violent sloshing even in low sea state. When the forcing frequencies are in the vicinity of the lowest natural frequency for the fluid motion inside a smooth tank, a violent free surface

wave may be observed even if the tank oscillates with a small amplitude. The resulting impact loads are also due to the violent free surface motion. These impact loads are of considerable concern and there is a great need for the calculation method to simulate the three dimensional flows with a violent free surface motion.

The computation of highly nonlinear free surface flows is difficult because neither the shape nor the position of the interface between air and water is known a priori; on the contrary, it often involves unsteady fragmentation and merging process. There are basically two approaches to compute flows with free surface: interface-tracking and interface-capturing methods. The former compute the liquid flow only, using a numerical grid that adapts itself to the shape and position of the free surface. The free surface is represented and tracked explicitly either by marking it with special marker points, or by attaching it to a mesh surface. Various surface fitting methods for attaching the interface to a mesh surface were developed during the past decades using the finite element method. In the interface tracking methods, the free surface is treated as a boundary of the computational domain, where the kinematic and dynamic boundary conditions are applied. These methods can not be used if the interface topology changes significantly (e.g. overturning or breaking waves).

On the other hand, interface-capturing methods consider both fluids as a single effective fluid with variable properties; the interface is captured as a region of sudden change in fluid properties. Either massless particles or an indicator function marks gas or fluid on either side of the interface. Among various interface-capturing methods, volume-of-fluid (VOF) methods and level-set (LS) methods are more economical than marker particles, as only one value (the volume fraction for VOF or the level-set function for LS) needs to be assigned to each mesh cell. Another benefit of using volume fractions or level-set functions is that only a scalar convection equation needs to be solved to propagate the volume fractions or level-set functions through the computational domain. The interface-capturing methods based on the Eulerian approach require no geometry manipulations after the mesh is generated and can be applied to interfaces of a complex topology

¹Cheung Kong Scholar, Shanghai Jiao Tong University.

such as overturning or breaking waves.

As the objective of this study is to model the highly nonlinear free surface flows, one of the most promising interface-capturing methods – VOF method is adopted and further developed. The VOF method was first reported in Nichols and Hirt (1975), and more completely in Hirt and Nichols (1981). This method has been improved in several aspects in the recent years (e.g. Scardovelli and Zaleski, 1999) and used to simulate breaking waves (e.g. Chen and Kharif, 1999; Biaisser et al., 2004), green water effects (e.g. Fekken et al., 1999; Huijsmans and van Groesen, 2004), and sloshing (e.g. Huijsmans et al., 2004). In the present study, an unstructured grid based solver for the incompressible Navier-Stokes equations has been extended to handle the highly nonlinear free surface flows via the VOF techniques. A fixed grid is used which covers the space occupied by both the liquid and the gas phase. Since the grid does not follow the deformation of the free surface, the grid movement is only necessary if the shape or location of the solid boundary changes (e.g. in the case of sloshing, slamming, floating bodies etc.). Only the liquid phase is simulated. An extrapolation algorithm is developed for obtaining the pressure and velocity in the gas region.

As one of the three-dimensional flows with violent free surface motion, numerical simulation of sloshing waves is considered in the present paper. Sloshing can occur in storage tanks, such as LNG tanks, aircraft and spacecraft fuel tanks. Large number of experimental and numerical studies on wave sloshing has been reported (e.g., Abramson et al., 1974; Sollas and Faltisen, 1997; Wu et al., 1998; Faltisen and Timokha, 2001; Kyoung et al., 2003; Landrini et al., 2003; Kim et al., 2003; Huijsmans et al., 2004). Many applications are given to the 2-D sloshing problems. In this work, both 2-D and 3-D sloshing problems are modeled and compared to one another.

In the following sections, we first briefly outline the basic elements of the present incompressible flow solver and the volume of fluid extensions. The computer code is then verified by comparing the calculated results with the published data for the classic breaking dam problem. After that, an extensive set of calculations is made for the sloshing of a partially filled two-dimensional tank due to sway excitation. The resulting wave heights and wave loads for various excitation frequencies and amplitudes are compared with experimental data and those predicted by the SPH method (Landrini et al., 2003). The numerical simulation of the sloshing of a partially filled three-dimensional tank at the is carried out and compared with its counterpart of a two-dimensional tank. It is particularly interesting to see that a three-dimensional partially filled tank undergoing sway motion in one direction induces a two-dimensional sloshing wave for the first 20 excitations and a steady three dimensional sloshing wave after that for the amplitude and frequency considered.

BASIC ELEMENTS OF THE SOLVER

The equations describing incompressible, Newtonian flows may be written as

$$\rho \mathbf{v}_{,t} + \rho \mathbf{v} \nabla \mathbf{v} + \nabla p = \nabla \mu \nabla \mathbf{v} + \rho \mathbf{g} \quad , \quad (1)$$

$$\nabla \cdot \mathbf{v} = 0 \quad . \quad (2)$$

Here ρ denotes the density, \mathbf{v} the velocity vector, p the pressure, μ the viscosity and \mathbf{g} the gravity vector. We remark that both

the gaseous and liquid phases are considered incompressible, thus Eqn.(2). The liquid-gas interface is described by a scalar equation of the form:

$$\Phi_{,t} + \mathbf{v} \cdot \nabla \Phi = 0 \quad . \quad (3)$$

For the classic VOF technique, Φ represents the total density of the material in a cell/element or control volume. For pseudo-concentration techniques, Φ represents the percentage of liquid in a cell/element or control volume. For the level set approach Φ represents the signed distance to the interface.

Since over a decade the numerical schemes chosen to solve the incompressible Navier-Stokes equations given by Eqns.(1,2) have been based on the following criteria:

- Spatial discretization using unstructured grids (in order to allow for arbitrary geometries and adaptive refinement);
- Spatial approximation of unknowns with simple finite elements (in order to have a simple input/output and code structure);
- Temporal approximation using implicit integration of viscous terms and pressure (the interesting scales are the ones associated with advection);
- Temporal approximation using explicit integration of advective terms;
- Low-storage, iterative solvers for the resulting systems of equations (in order to solve large 3-D problems); and
- Steady results that are independent from the timestep chosen (in order to have confidence in convergence studies).

A detailed description of the numerical solution procedure can be found in authors' previous work (Löhner, 1990; Löhner et al., 1998; Yang and Löhner, 1998; Löhner et al., 1999; Löhner, 2004).

VOLUME OF FLUID EXTENSIONS

The extension of a solver for the incompressible Navier-Stokes equations to handle free surface flows via the VOF or level set techniques requires a series of extensions which are the subject of the present section.

Extrapolation of the Pressure

The pressure in the gas region needs to be extrapolated properly in order to obtain the proper velocities in the region of the free surface. This extrapolation is performed using a three step procedure. In the first step, the pressures for all points in the gas region are set to (constant) values, either the atmospheric pressure or, in the case of bubbles, the pressure of the particular bubble. In the second step, the gradient of the pressure for the points in the liquid that are close to the liquid-gas interface are extrapolated from the points inside the liquid region (see Figure 1). This step is required as the pressure gradient for these points can not be computed properly from the data given. Using this information (i.e. pressure and gradient of pressure), the pressure for the points

in the gas that are close to the liquid-gas interface are computed.

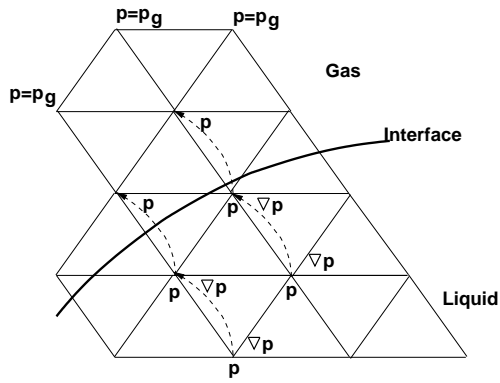


Figure 1: Extrapolation of the Pressure

Extrapolation of the Velocity

The velocity in the gas region needs to be extrapolated properly in order to propagate accurately the free surface. This extrapolation is started by initializing all velocities in the gas region to $\mathbf{v} = 0$. Then, for each subsequent layer of points in the gas region where velocities have not been extrapolated (unknown values), an average of the velocities of the surrounding points with known values is taken (see Figure 2).

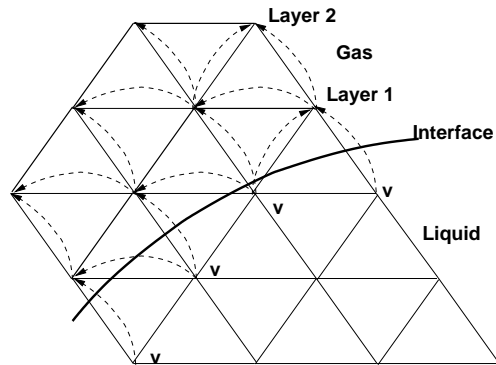


Figure 2: Extrapolation of the Velocity

Imposition of Constant Mass

Experience indicates that the amount of liquid mass (as measured by the region where the VOF indicator is larger than a cut-off value) does not remain constant for typical runs. The reasons for this loss or gain of mass are manifold: loss of steepness in the interface region, inexact divergence of the velocity field, boundary velocities, etc. This lack of exact conservation of liquid mass has been reported repeatedly in the literature. The recourse taken here is the classic one: add/remove mass in the interface region in order to obtain an exact conservation of mass. At the end of every timestep, the total amount of fluid mass is compared to the expected value. The expected value is determined from the mass at the previous timestep, plus the mass-flux across all boundaries during the timestep. The differences in expected and actual mass are typically very small, so that quick convergence is achieved by simply adding and removing mass appropriately. The amount of mass taken/added is made proportional to the absolute value of

the normal velocity of the interface:

$$v_n = \left| \mathbf{v} \cdot \frac{\nabla \Phi}{|\nabla \Phi|} \right|. \quad (4)$$

In this way the regions with no movement of the interface remain unaffected by the changes made to the interface in order to impose strict conservation of mass.

Deactivation of Air Region

Given that the air region is not treated/updated, any CPU spent on it may be considered wasted. Most of the work is spent in loops over the edges (upwind solvers, limiters, gradients, etc.). Given that edges have to be grouped in order to avoid memory contention/ allow vectorization when forming right-hand sides (Löhner, 1993, Löhner, 1998), this opens a natural way of avoiding unnecessary work: form relatively small edge-groups that still allow for efficient vectorization, and deactivate groups instead of individual edges (Löhner, 2001). In this way, the basic loops over edges do not require any changes. The if-test whether an edge group is active or inactive occurs outside the inner loops over edges, leaving them unaffected. On scalar processors, edge-groups as small as $n_{\text{grp}}=8$ are used. Furthermore, if points and edges are grouped together in such a way that proximity in memory mirrors spatial proximity, most of the edges in air will not incur any CPU penalty.

NUMERICAL RESULTS

In the following examples, the fluid is assumed to be a laminar Newtonian fluid with reference viscosity $\mu = 0.01$. The free slip condition is imposed on the solid boundaries. The numerical force is calculated by integrating the pressure force.

Breaking Dam Problem

This is a classic test case for free surface flows. The problem definition is shown in Figure 4a.

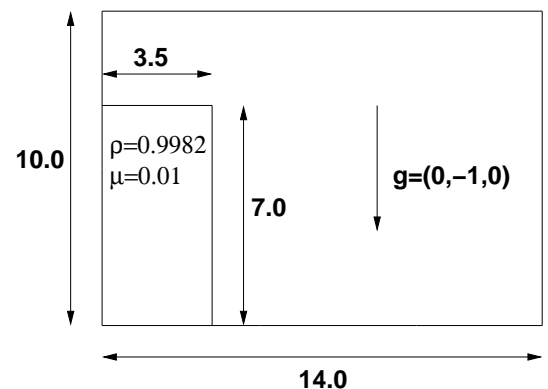


Figure 4a: Breaking Dam: Problem Definition

This case was run on a coarse mesh with $n_{\text{elem}}=16,562$ elements, a fine mesh with $n_{\text{elem}}=135,869$ and an adaptively refined mesh (where the coarse mesh was the base mesh) with approximately $n_{\text{elem}}=30,000$ elements. The refinement indicator for the latter was the free surface, and the mesh was adapted every 5 time steps. Figure 4b shows the discretization for the coarse

mesh. The results obtained for the horizontal location of the free surface along the bottom wall are compared to the experimental values of Martin and Moyse (1952), as well as the numerical results obtained by Hansbo (1992), Kölke (2005), Walhorn (2002) in Figure 4c. The dimensionless time and displacement are given by $\tau = t\sqrt{2g/a}$ and $\delta = x/a$. As one can see, the agreement is very good, even for the coarse mesh. The difference between the adaptively refined mesh and the fine mesh was almost indistinguishable, and therefore only the results for the fine mesh are shown in the graph. Figure 4d shows the flow field and free surface at a given time $t = 3$.

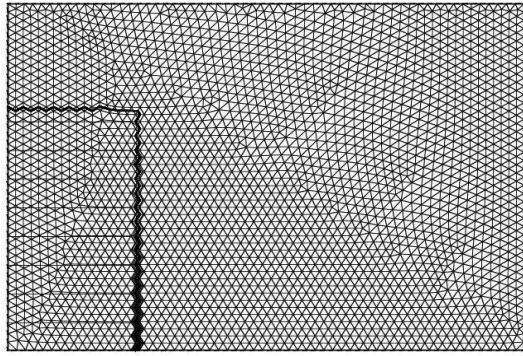


Figure 4b: Breaking Dam: Discretization for the Coarse Mesh

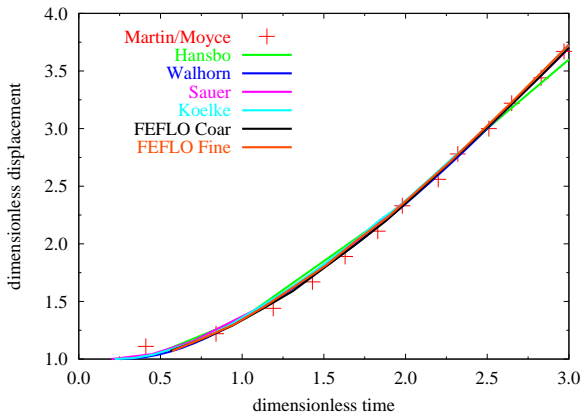


Figure 4c: Breaking Dam: Horizontal Displacement

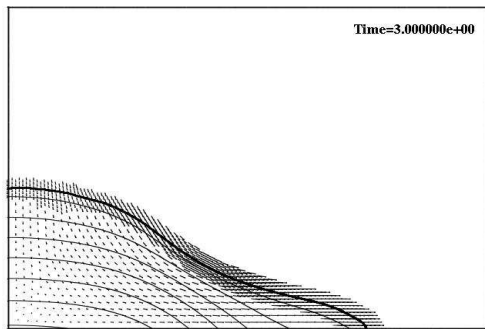


Figure 4d: Breaking Dam: Flowfield at $t=3$.

Sloshing of a 2D Tank due to Sway Excitation

In the previous section, we have already verified the accuracy of our numerical model for studying wave breaking. In this section, we shall apply our numerical model to study the sloshing of a partially filled 2D tank. The main tank dimensions are $L = H = 1m$, with tank width $b = 0.1m$. The problem definition is shown in Figure 5a. This case is run on a mesh with $nelem=54,124$ elements.

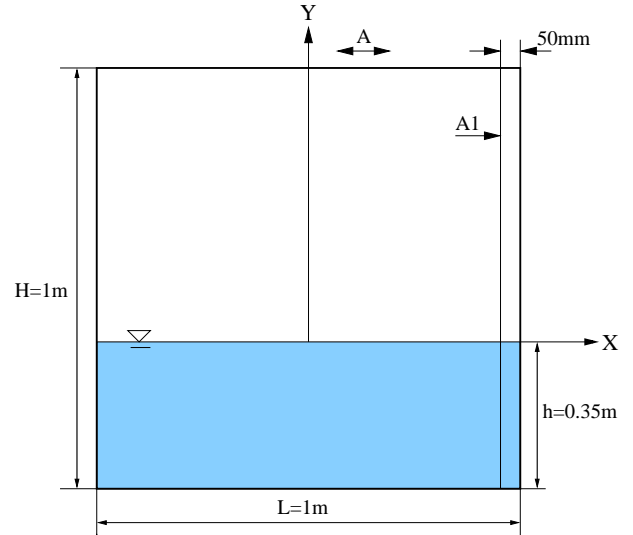


Figure 5a: 2D Tank: Problem Definition

Experimental data for the above tank with a filling level $h/L = 0.35$ have been provided by Olsen (1970), and reported in Faltsen (1974) and Olsen and Johnsen (1975), where the tank was undergoing a sway motion, i.e., the tank oscillates horizontally with law $A\sin(2\pi t/T)$. A wave gage was placed $0.05m$ from the right wall and the maximum wave elevation relative to a tank-fixed coordinate system was recorded. In the numerical simulations reported by Landrini et al. (2003) using the SPH method, the forced oscillation amplitude increases smoothly in time and reaches its steady regime value in $10T$. The simulation continues for another $30T$, and the maximum wave elevation is recorded in last 10 periods of oscillation.

We followed the same procedure as Landrini et al. (2003) in our numerical simulation for 32 cases, which correspond to 2 amplitudes ($A = 0.025, 0.05$) and 16 periods, ranging from $T = 1 - 1.8$ seconds or $T/T_1 = 0.787 - 1.42$, where $T_1 = 1.27$ seconds. When $h/L = 0.35$ the primary resonances of the first and the third modes occur at $T/T_1 = 1$ and $T/T_1 = 0.55$, respectively. The secondary resonance of the second mode is at $T/T_1 = 1.28$ (see Landrini et al. 2003).

The present VOF results for the time history of the lateral force F_x when $T = 1.2, 1.3$ and $A = 0.025, 0.05$ are shown in Figure 5b. The corresponding time history of the wave elevation at the wave probe A1 (see Figure 5a) are shown in Figure 5c. Some free surface snapshots are shown in Figure 5d.

The present VOF results for maximum wave elevation ζ at the wave probe A1 (see Figure 5a) are compared with the experimental data and SPH results (Landrini et al. 2003) in Figures 5e for

$A/L = 0.025, 0.05$. The predicted lateral absolute values of maximum forces are compared with the experimental data and SPH results (Landrini et al. 2003) in Figure 5f for $A/L = 0.05$ (There is no force data available for $A/L = 0.025$). Figure 5g shows the comparison of predicted lateral absolute values of maximum forces for $A/L = 0.025, 0.05$. It can be seen from Figures 5e-f that both maximum wave height and lateral absolute values of maximum forces predicted by present VOF method agrees fairly well with the experimental data and SPH results except there is a small phase shift among three results.

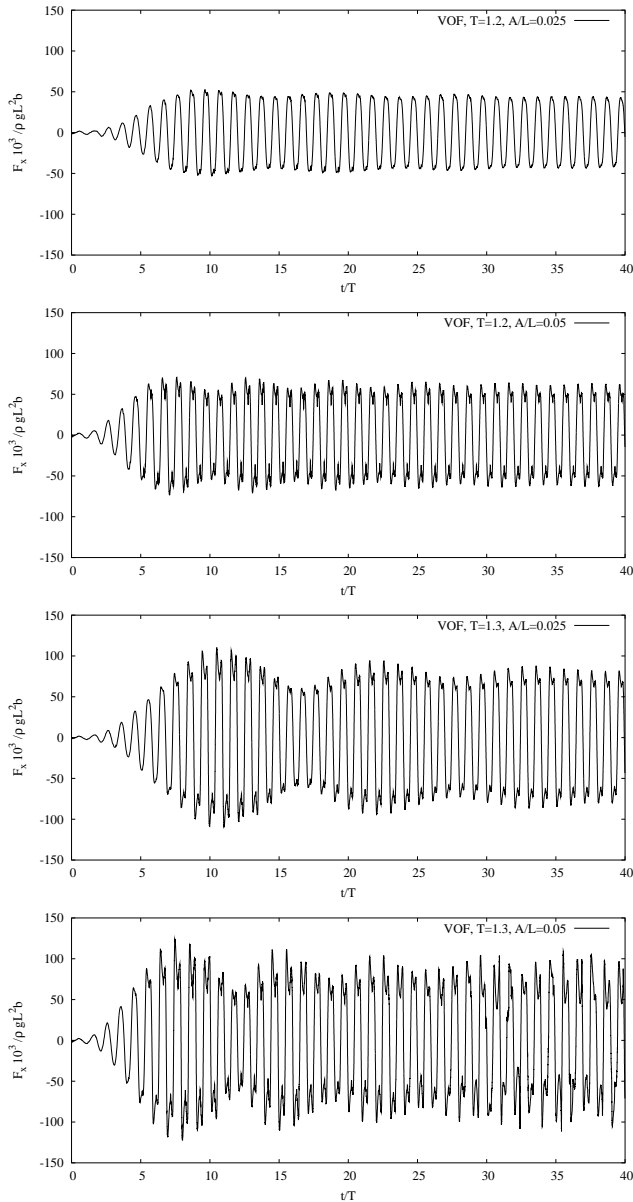


Figure 5b: 2D Tank: Time History of Lateral Force F_x

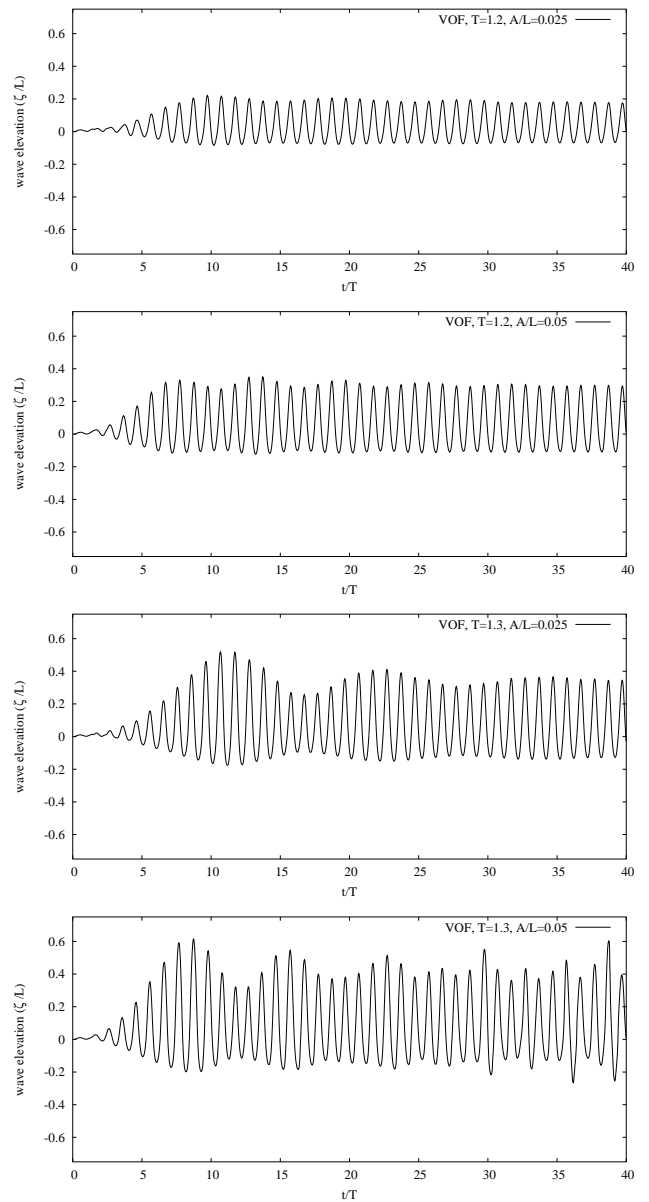


Figure 5c: 2D Tank: Time History of Wave Elevation at the Wave Probe A1

Figures 5b and 5c are typical time history plots. It should be noted from these figures that even after a long simulation time (40 periods), steady state results are not generally obtained. This is due to very small damping in the system. Landrini et al. (2003) noted the same behavior in their numerical simulations. As a result, the predicted maximum wave elevation and the lateral absolute values of maximum forces plotted in Figure 5e are average maximum values for the last few periods for the cases when the steady state is not reached.

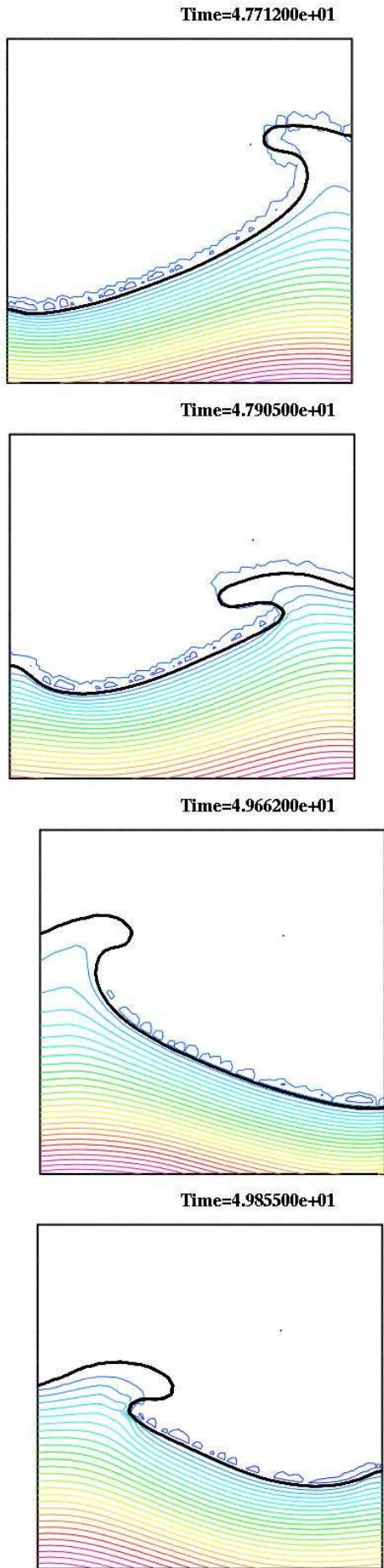


Figure 5d: 2D Tank: Snapshots of Free Surface Wave Elevation for $T = 1.3$ and $A/L = 0.05$

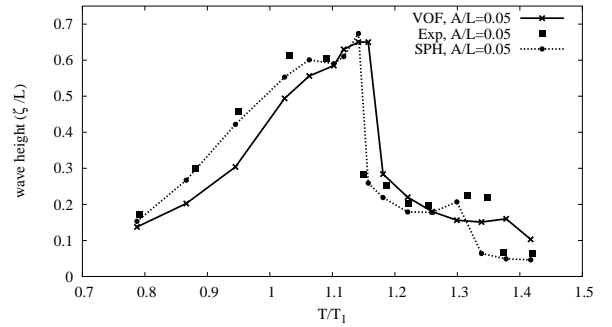
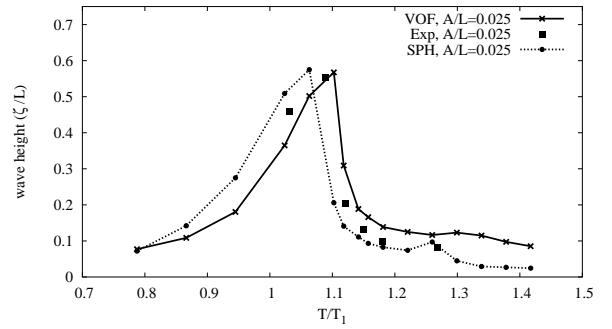


Figure 5e: 2D Tank: Maximum Wave Height at the Wave Probe A1

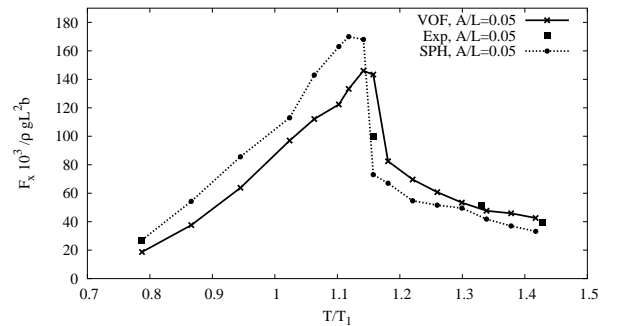


Figure 5f: 2D Tank: Maximum Absolute Values of Lateral Force F_x for $A/L = 0.05$

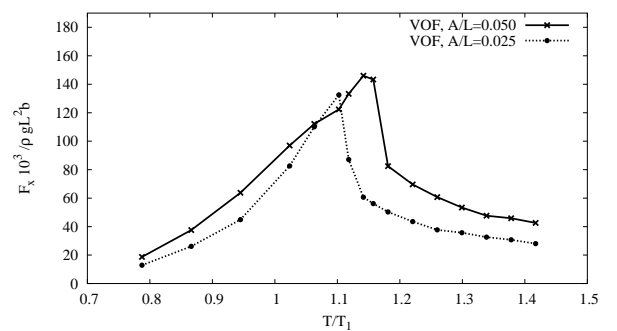


Figure 5g: 2D Tank: Predicted Maximum Absolute Values of Lateral Force F_x for $A/L = 0.025, 0.05$

Sloshing of a 3D Tank due to Sway Excitation

In order to study the three dimensional effects, the sloshing of a partially filled 3D tank is then considered. The main tank dimensions are $L = H = 1m$, with tank width $b = 1m$. The problem definition is shown in Figure 6a. The 3D tank has the same filling

level $h/L = 0.35$ as the 2D tank. The 3D tank case is run on a mesh with $n_{elem}=561,808$ elements, and the 2D tank is run on a mesh with $n_{elem}=54,124$ elements.

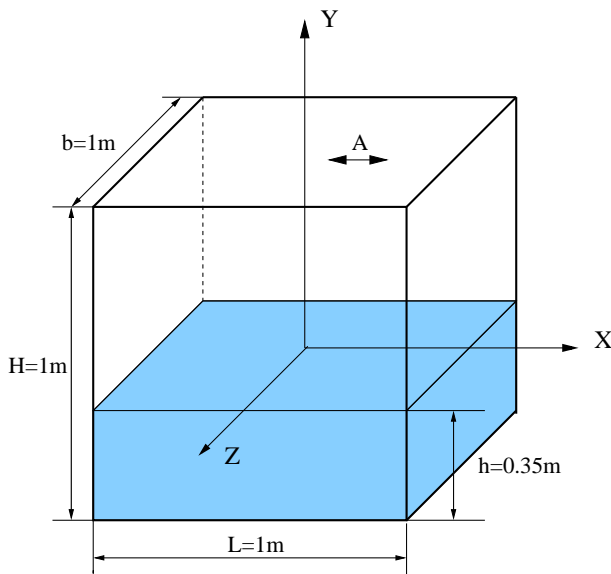


Figure 6a: 3D Tank: Problem Definition

The numerical simulations are carried out for both 3D and 2D tanks, where both tanks are undergoing the prescribed sway motion, i.e., the tanks oscillate horizontally with law $A \sin(2\pi t/T)$. The simulations were carried out for $A = 0.025$ and $T = 1.27$ or $T/T_1 = 1$. The forced oscillation amplitude increases smoothly in time and reaches its steady regime value in $10T$. The simulation continues for another $70T$.

In order to show the 3D effects, the forces are nondimensionalized with $\rho g L^2 b$ for both 2D and 3D tanks. Figures 6b,c show the time history of the force F_x (horizontal force in the same direction as the tank moving direction) for both 2D and 3D tanks. Figure 6d shows the time history of the force F_z (horizontal force perpendicular to the tank moving direction) for 3D tank. It is very interesting to observe from Figures 6c,d that there are almost no 3D effects for the first 25 oscillating periods. The 3D modes start to appear after $25T$, and fully build up at about $40T$. The 3D flow pattern then remains steady and periodic for the rest of the simulation, which is about 40 more oscillating periods.

Figures 7a-c show a sequence of snapshots of the free surface wave elevation for the 3D tank. For the first set of snapshots (see Figure 7a), the flow is still two-dimensional. The 3D flow starts to build up in the second set of snapshots (see Figure 7b). The flow remains periodic three-dimensional for the last 40 periods. Figure 7c show the typical snapshots of the free surface for the last 40 periods. The 3D effects are clearly shown in these plots. Figure 8 show a sequence of snapshots of the free surface wave elevation for the 2D tank at the same time instance as those shown in Figure 7a. The flow remains periodic two-dimensional for the rest of the simulation.

CONCLUSIONS

A robust Volume of Fluid (VOF) technique has been developed and coupled with an incompressible Euler/Navier Stokes solver operating on adaptive, unstructured grids to simulate the interactions of extreme waves and three-dimensional structures. In the present approach, only the liquid phase needs to be simulated. An effective extrapolation technique has been developed to obtain the pressure and velocity in the gas region.

In this study, the classic breaking dam problem has been used to verify the computer code. The results obtained for the horizontal location of the free surface along the bottom wall are compared to the experimental values and other numerical predictions. The agreement is very good, even for the coarse mesh.

An extensive set of calculations is then performed for the sloshing of a partially filled 2D tank due to sway excitation. The resulting wave heights and wave loads for various excitation frequencies and amplitudes are compared with experimental data and those predicted by the SPH method (Landrini et al., 2003). The agreement is fairly well. Finally, the numerical simulation of the sloshing of a partially filled 3D tank is carried out and compared with its counterpart of a 2D tank. It is particularly interesting to see that a 3D partially filled tank undergoing sway motion in one direction induces a two-dimensional sloshing wave for the first 20 excitations and a steady three dimensional sloshing wave after that.

Computational results have demonstrated that the present CFD method is capable of simulating the 3D flows with a violent free surface motion, which is of great importance to the offshore and shipping industry.

ACKNOWLEDGMENTS

The authors wish to thank Mr. Andrea Colagrossi of the INSEAN for providing both experimental data and numerical results for the sloshing of a 2D tank.

REFERENCES

- Abramson, H.N., 1996, "The dynamic Behaviour of Liquid in Moving Containers," Reports SP 106 of NASA.
- Alessandrini, B. and Delhommeau, G., 1996, "A Multigrid Velocity- Pressure-Free Surface Elevation Fully Coupled Solver for Calculation of Turbulent Incompressible Flow Around a Hull," Proc. 21st Symp. on Naval Hydrodynamics, Trondheim, Norway, June.
- Bell, J.B., Colella, P. and Glaz, H., 1989, "A Second-Order Projection Method for the Navier-Stokes Equations," J. Comp. Phys. 85, 257-283.
- Bell, J.B. and Marcus, D.L., 1992, "A Second-Order Projection Method for Variable-Density Flows," J. Comp. Phys. 101, 2.
- Biausser, B., Fraunie, P., Grilli, S. and Marcer R., 2004, "Numerical analysis of the internal kinematics and dynamics of three-dimensional breaking waves on slopes," International Journal of Offshore and Polar Engineering, Vol. 14, No. 4.
- Chen, G., Kharif, C., 1999, "Two-Dimensional Navier-Stokes Simulation of Breaking Waves," Physics of Fluids, 11(1), 121-133.

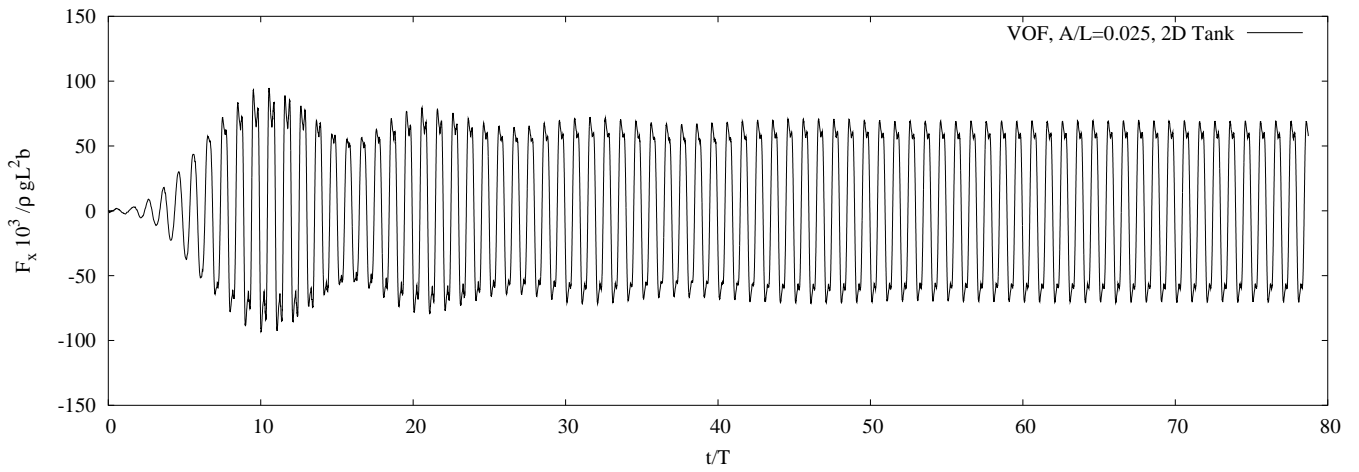


Figure 6b: 3D Tank: Time History of Force F_x for a 2D Tank at $A/L = 0.025, T/T_1 = 1)$

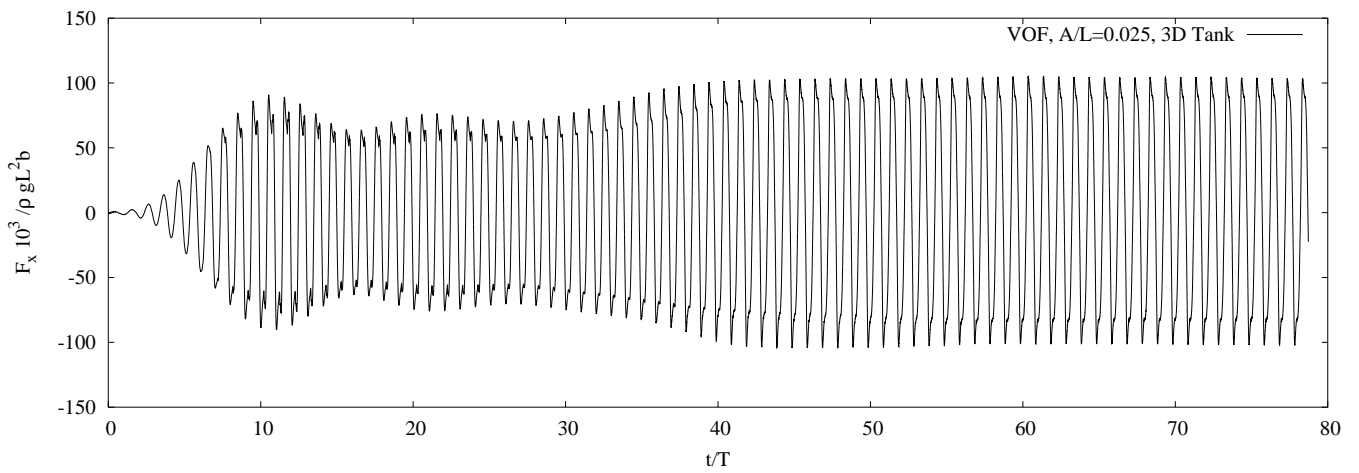


Figure 6c: 3D Tank: Time History of Force F_x for a 3D Tank at $A/L = 0.025, T/T_1 = 1)$

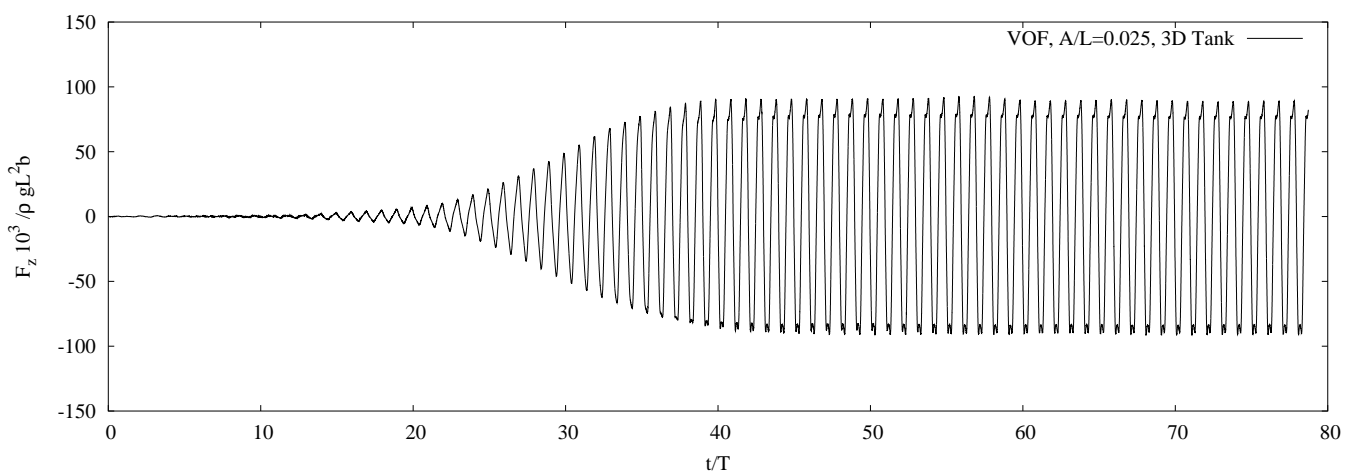


Figure 6d: 3D Tank: Time History of Force F_z for a 3D Tank at $A/L = 0.025, T/T_1 = 1)$

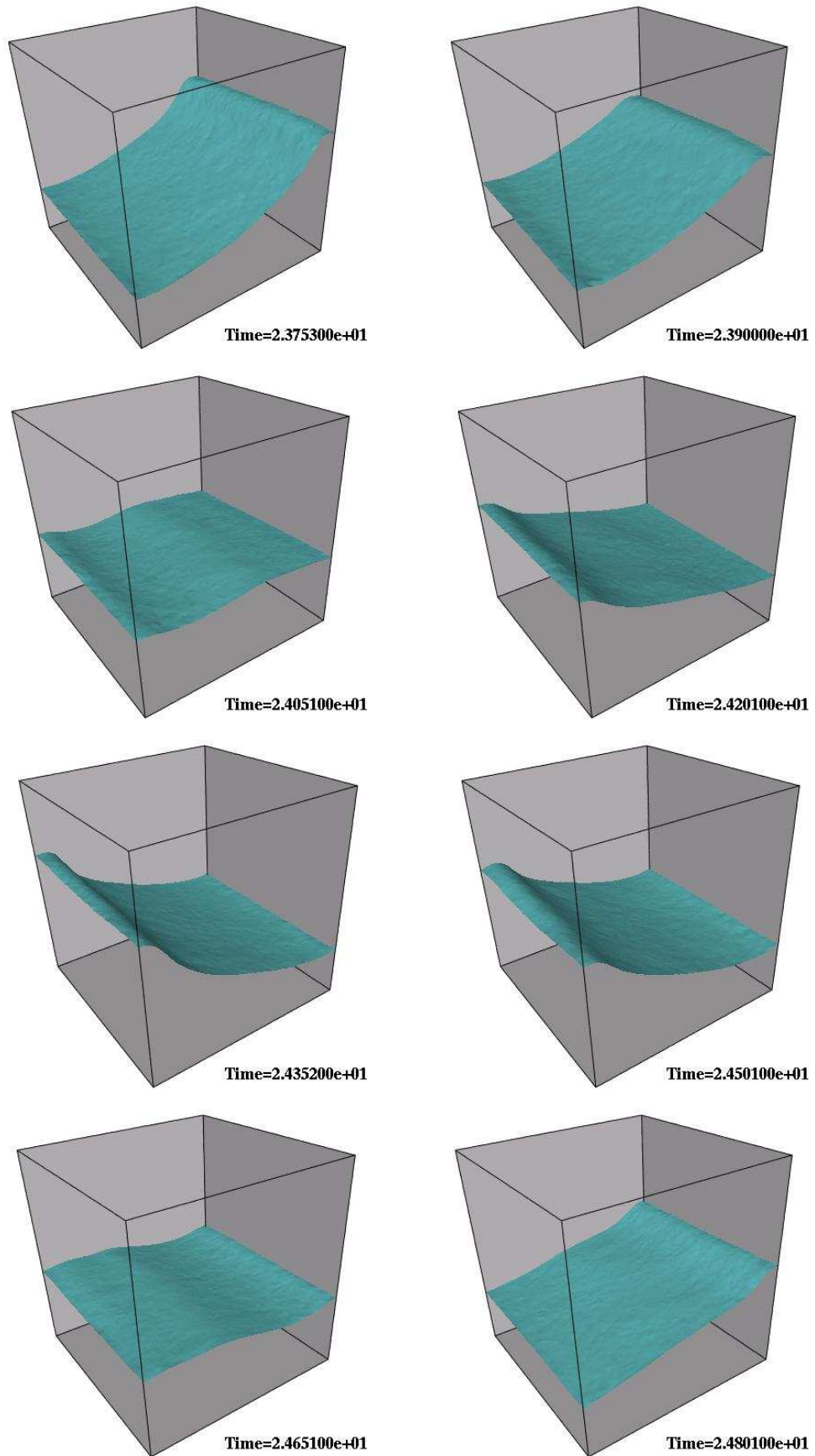


Figure 7a: Snap Shots of the Free Surface Wave Elevation for 3D Tank

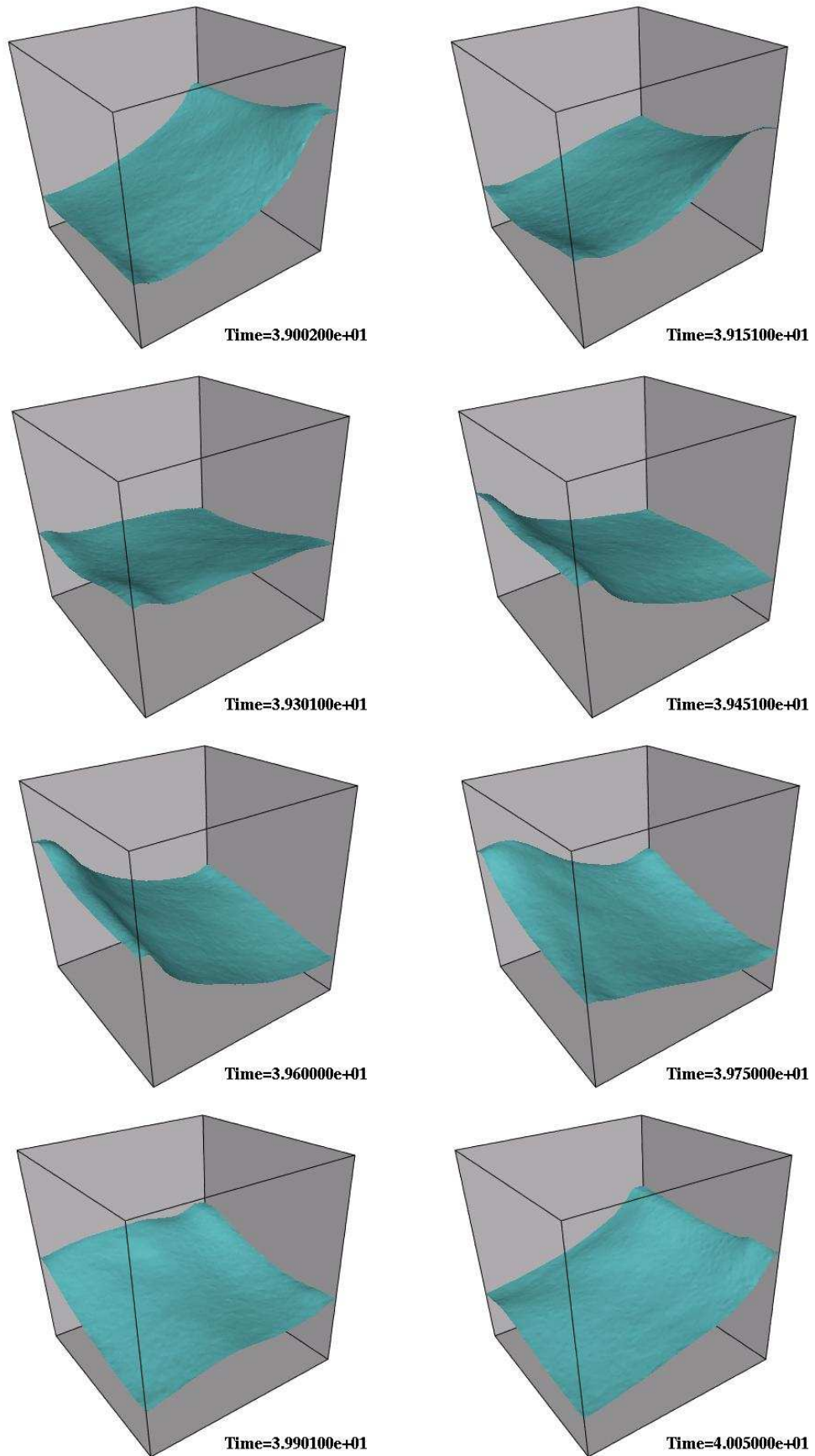


Figure 7b: Snap Shots of the Free Surface Wave Elevation for 3D Tank

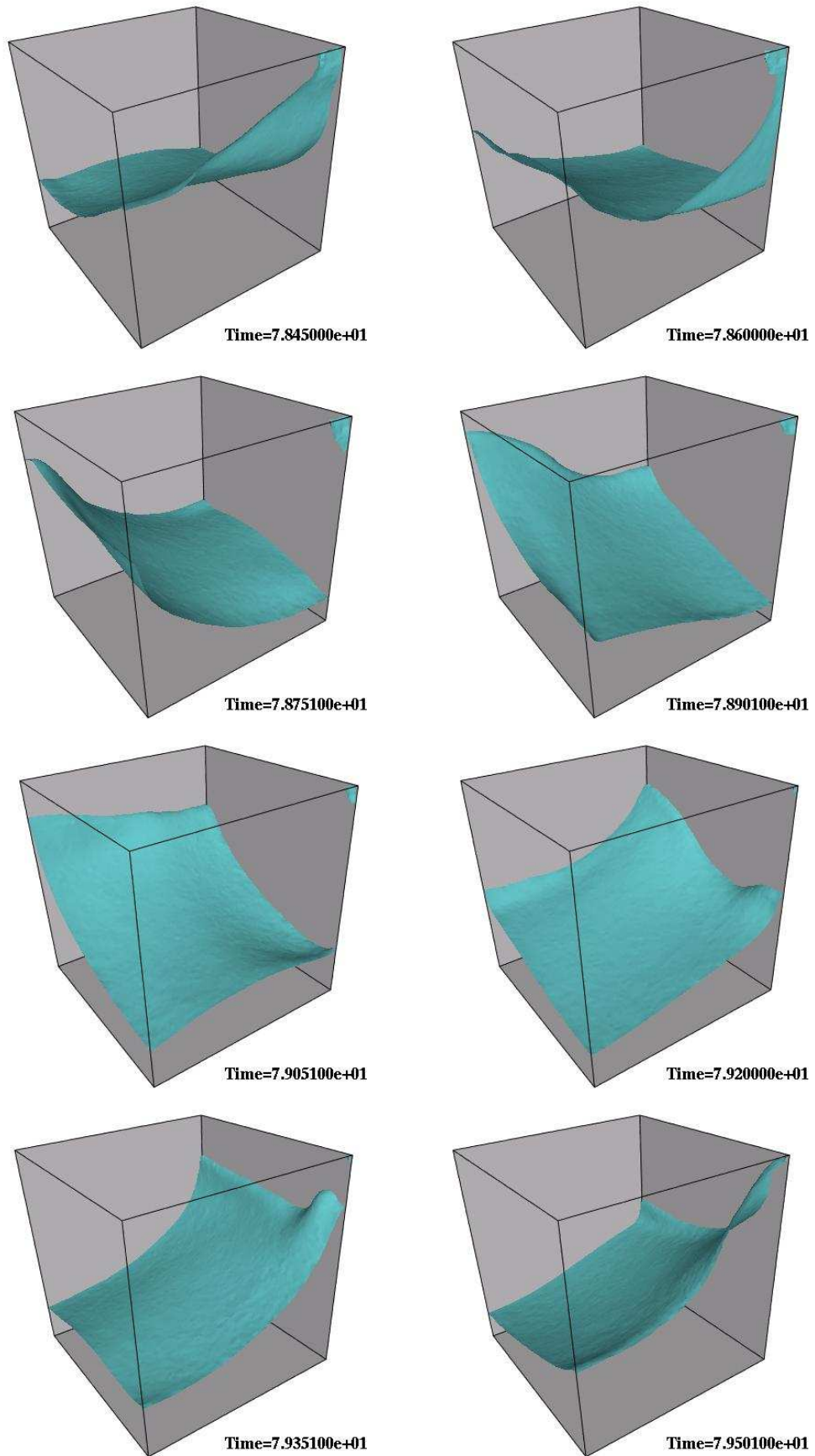


Figure 7c: Snap Shots of the Free Surface Wave Elevation for 3D Tank

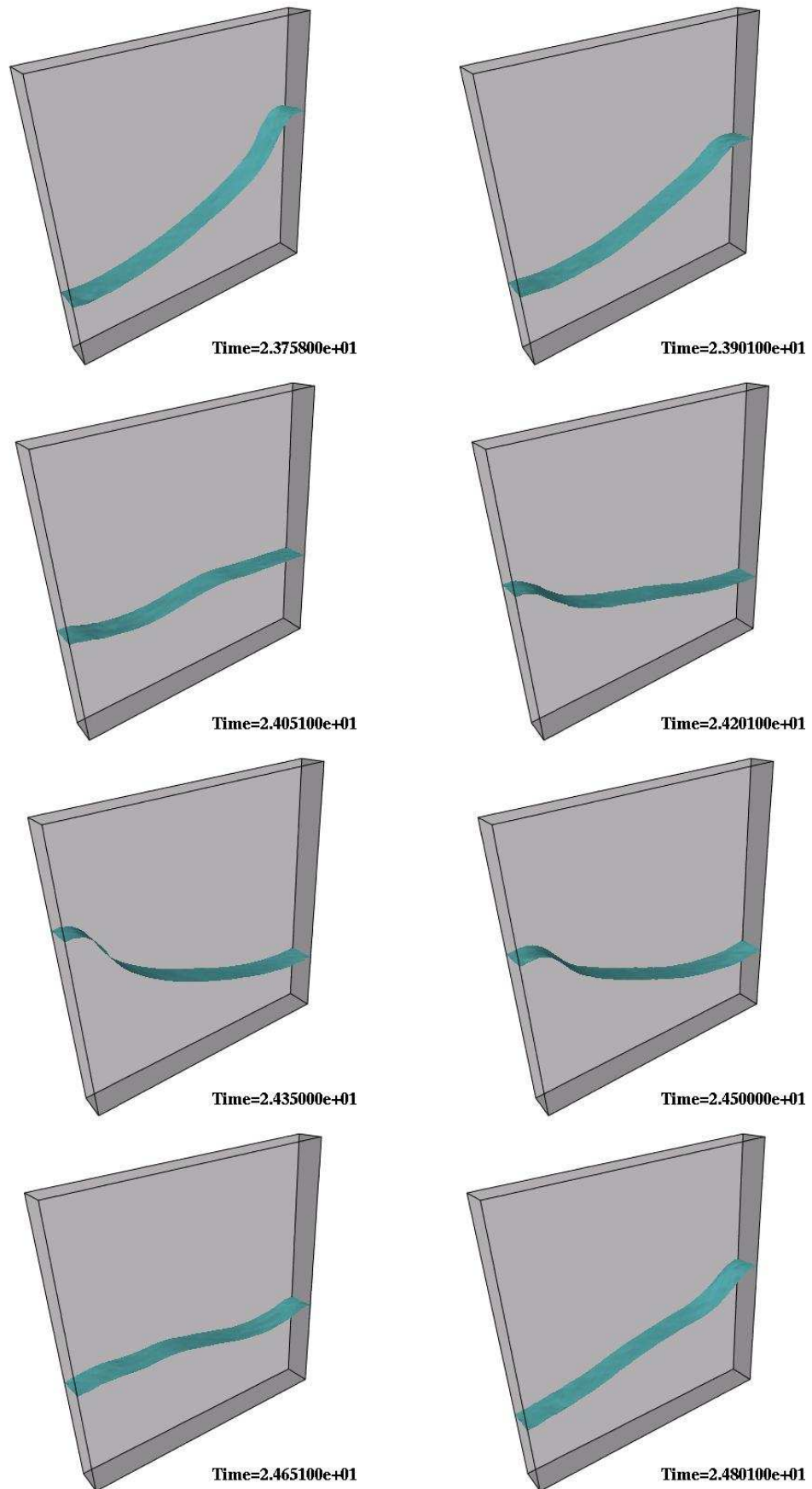


Figure 8: Snap Shots of the Free Surface Wave Elevation for 2D Tank

- Codina, R., 2001, "Pressure Stability in Fractional Step Finite Element Methods for Incompressible Flows," *J. Comp. Phys.* 170, 112-140.
- Faltisen, O.M., 1974, "A Nonlinear Theory of Sloshing in Rectangular Tanks," *Journal of Ship Research*, 18/4, pp. 224-241.
- Faltisen, O.M. and Timokha A.N., 2001, "Adaptive Multimodal Approach to Nonlinear Sloshing in a Rectangular Tank," *Journal of Fluid Mechanics*, Vol. 432, pp. 167-200.
- Fekken, G., Veldman, A.E.P. and Buchner, B., 1999, "Simulation of Green Water Loading Using the Navier-Stokes Equations," *Proceedings of the 7th International Conference on Numerical Ship Hydrodynamics*, Nantes, France.
- Hansbo, P., 1992, "The Characteristic Streamline Diffusion Method for the Time-Dependent Incompressible Navier-Stokes Equations," *Comp. Meth. Appl. Mech. Eng.* 99, 171-186.
- Hirt, C.W. and Nichols, B.D., 1981, "Volume of Fluid (VOF) Method for the Dynamics of Free Boundaries," *Journal of Computational Physics* 39, 201.
- Huijsmans, R.H.M. and van Groenou, E., 2004, "Coupling Freak Wave Effects with Green Water Simulations," *Proceeding of the 14th ISOPE*, Toulon, France, May 23-28.
- Kallinderis, Y. and Chen, A., 1996, "An Incompressible 3-D Navier-Stokes Method with Adaptive Hybrid Grids," *AIAA-96-0293*.
- Karbon, K.J. and Kumarasamy, S., 2001, "Computational Aeroacoustics in Automotive Design, Computational Fluid and Solid Mechanics," *Proc. First MIT Conference on Computational Fluid and Solid Mechanics*, 871-875, Boston.
- Karbon, K.J. and Singh, R., 2002, "Simulation and Design of Automobile Sunroof Buffeting Noise Control," *8th AIAA-CEAS Aero-Acoustics Conf.*, Breckenridge.
- Kim, J. and Moin, P., 1985, "Application of a Fractional-Step Method to Incompressible Navier-Stokes Equations," *J. Comp. Phys.* 59, 308-323.
- Kim, Y., Shin, Y.-S., Lin, W.-M., and Yue, D.K.P., 2003, "Study on Sloshing Problem Coupled with Ship Motion in Waves," *em Proceeding of the 8th International Conference on Numerical Ship Hydrodynamics*, Busan, Korea.
- Kölke, A., 2005, "Modellierung und Diskretisierung bewegter Diskontinuitäten in Randgekoppelten Mehrfeldaufgaben," *Ph.D. Thesis*, TU Braunschweig.
- Kyoung, J.H., Kim, J.W. and Bai, K.J., 2003, "A Finite Element Method for a Nonlinear Sloshing Problem," *em Proceeding of the OMAE Conference*, Cancun, Mexico.
- Li, Y., Kamioka, T., Nouzawa, T., Nakamura, T., Okada, Y. and Ichikawa, N., 2002, "Verification of Aerodynamic Noise Simulation by Modifying Automobile Front-Pillar Shape," *JSAE 20025351, JSAE Annual Conf.*, Tokyo, Japan.
- Landrini, M., Colagorossi, A. and Faltisen, O.M., 2003, "Sloshing in 2-D Flows by the SPH Method," *Proceeding of the 8th International Conference on Numerical Ship Hydrodynamics*, Busan, Korea.
- Löhner, R., 1990, "A Fast Finite Element Solver for Incompressible Flows," *AIAA-90-0398*.
- Löhner, R. 1993, "A Fast Finite Element Solver for Incompressible Flows," *AIAA-90-0398*.
- Löhner, R., 1998, "Renumbering Strategies for Unstructured-Grid Solvers Operating on Shared-Memory, Cache-Based Parallel Machines," *Comp. Meth. Appl. Mech. Eng.* 163, 95-109.
- Löhner, R., Yang, C., Oñate, E. and Idelsohn, S., 1999, "An Unstructured Grid-Based, Parallel Free Surface Solver," *Appl. Num. Math.* 31, 271-293.
- Löhner, R. 2001, *Applied CFD Techniques*; J. Wiley & Sons.
- Löhner, R., 2004, "Multistage Explicit Advective Prediction for Projection-Type Incompressible Flow Solvers," *J. Comp. Phys.* 195, 143-152.
- Martin, D. and Löhner, R., 1992, "An Implicit Linelet-Based Solver for Incompressible Flows," *AIAA-92-0668*.
- Martin, J.C. and Moyce, W.J., 1952, "An Experimental Study of the Collapse of a Liquid Column on a Rigid Horizontal Plane," *Phil. Trans. Royal Soc. London A244*, 312-324.
- Nichols, B.D. and Hirt, C.W., 1975, "Methods for Calculating Multi-Dimensional, Transient Free Surface Flows Past Bodies," *Proc. First Intern. Conf. Num. Ship Hydrodynamics*, Gaithersburg, MD, Oct. 20-23.
- Olsen, H., 1970, "Unpublished Sloshing Experiments at the Technical University of Delft," Delft, The Netherlands.
- Olsen, H. and Johnsen, K.R., 1975, "Nonlinear Sloshing in Rectangular Tanks. A Pilot Study on the Applicability of Analytical Models," *Det Norske Veritas Report 74-72-S*, Vol. II.
- Ramamurti, R. and Löhner, R., 1996, "A Parallel Implicit Incompressible Flow Solver Using Unstructured Meshes," *Computers and Fluids* 5, 119-132.
- Sollas, F. and Faltisen, O.M., 1997, "Sloshing in Two-Dimensional Tanks," *Weinblum Meeting*, 12th International Workshop on Water Waves and Floating Bodies, Carry-le-Rouet, France, March.
- Scardovelli, R.; Zaleski, S., 1999, "Direct numerical simulation of free-surface and interfacial flow," *Annual Review of Fluid Mechanics* 31: 567-603.
- Takamura, A., Zhu, M. and Vinteler, D., 2001, "Numerical Simulation of Pass-by Maneuver Using ALE Technique," *JSAE Annual Conf.*, Tokyo, Japan.
- Walhorn, E., 2002, "Ein Simultanes Berechnungsverfahren für Fluid-Struktur-Wechselwirkungen mit Finiten Raum-Zeit-Elementen," *Ph.D. Thesis*, TU Braunschweig.
- Wu, G.X., Ma, Q.W. and Eatock Taylor, R., 1998, "Numerical Simulation of Sloshing Waves in a 3D Tank Based on a Finite Element Method," *Applied Ocean Research*, 20, pp. 337-355.
- Yang, C. and Löhner, R., 1998 "Fully Nonlinear Ship Wave Calculation Using Unstructured Grids and Parallel Computing," *Proc. 3rd Osaka Colloquium on Advanced CFD Applications to Ship Flow and Hull Form Design*, Osaka, Japan.